JOURNAL OF Materials CHEMISTRY

Effect of temperature on cation disorder in $ABi_2Nb_2O_9$ (A = Sr, Ba)

Ismunandar and Brendan J. Kennedy*

School of Chemistry, F11, The University of Sydney, Sydney, NSW 2006, Australia.
E-mail: Kennedyb@chem.usyd.edu.au

Received 28th August 1998, Accepted 11th November 1998

The influence of thermal annealing on cation disorder in $ABi_2Nb_2O_9$ (A = Sr, Ba) has been studied using synchrotron powder X-ray diffraction methods. $BaBi_2Nb_2O_9$ adopts a tetragonal ($I4_1/mmm$) structure, whilst $SrBi_2Nb_2O_9$ is orthorhombic, space group $A2_1am$, irrespective of the annealing conditions. In both complexes the A-type cations, Sr and Ba, are disordered over the perovskite and Bi_2O_2 layers. Quenching the samples from high temperature results in a slight increase in both the cell volume and the degree of disorder, the extent of disorder being greater in the Ba complex. Variable temperature diffraction studies are also reported.

Introduction

Recent structural studies on the Aurivillius type compounds $ABi_2Nb_2O_9$ (A = Sr, Ba) gave contradictory results.[1,2] Using powder neutron diffraction data Ismunandar *et al.* reported that there was no cation disorder in these oxides,[1] conversely using a combination of powder neutron and X-ray diffraction data Blake *et al.* found a small amount of disorder of the A and Bi cations in these systems and they postulated that the observed differences between the two studies may have resulted from the differing annealing conditions used in the two studies.[2]

The interest in these oxides is a result of their potential technological importance for a diverse range of applications including ferroelectric materials, catalysts for the selective oxidation and ammoxidation of olefins, and as fast ion conductors.[3–5] Aurivillius compounds, with the general formula $Bi_2A_{m-1}B_mO_{3m+3}$ ($m = 1,2,3,4$) are composed of two structural elements, α-PbO-type $[Bi_2O_2]^{2+}$ layers and perovskite-type layers having the composition $[A_{m-1}B_mO_{3m-1}]^{2-}$.[6] Most of the $m = 2$ oxides, with the general formula $ABi_2B_2O_9$, exhibit small distortions resulting in orthorhombic symmetry, although some adopt the archetypal $I4_1/mmm$ tetragonal structure.

The desirable physical and electronic properties of Aurivillius type oxides can in principle be tailored by varying the metal cation stoichiometry. A number of cations including Ca, Sr, Ba, Pb, Bi, Na, rare-earth ions, or mixtures of these have been used as A-type cations, while small highly charged cations such as Ti^{4+}, Nb^{5+}, Ta^{5+}, W^{6+}or Mo^{6+} can be added to the B type sites. In comparison to the ease of substitution into the perovskite layers early studies suggested substitution into the $[Bi_2O_2]^{2+}$ layers was not possible.[7,8] These layers have a square planar net of oxygen anions with the Bi^{3+} cations alternatively above and below the plane formed by Bi capped BiO_4 square pyramids. The Bi $6s^2$ lone pair electrons are stereochemically active and this is believed to limit substitution into the $[Bi_2O_2]^{2+}$ layers. Recently other cations with lone pair electrons including Sn^{2+}, Sb^{3+}, Pb^{2+} and Te^{4+} have been introduced into the Bi_2O_2 layers.[9–13]

Recently we reported a study of thermally induced cation disorder in $PbBi_2Nb_2O_9$.[14] This study highlighted a number of problems with the use of combined X-ray and neutron diffraction data, arising in particular from the similarity in the neutron scattering power of Pb and Bi. In this previous work we noted that simulations of the neutron diffraction data, which are relatively insensitive to the distribution of Pb^{2+} and Bi^{2+}cations, and the X-ray diffraction data significantly increased the uncertainty in the refined occupancies and this precluded a meaningful analysis. It is also well recognised that in powder diffraction a model that satisfactorily reproduces multiple diffraction data sets is more likely to be accurate.[15] These observations prompted us to exploit the ability of synchrotron radiation to record high quality diffraction data at multiple wavelengths, and thus of scattering powers, in order to (1) verify the presence of cation disorder in $ABi_2Nb_2O_9$ (A = Sr, Ba), and (2) investigate the effect thermal annealing has on the structures of these complex oxides.

Experimental

$ABi_2Nb_2O_9$ (A = Sr, Ba) were prepared by the solid state reaction of $SrCO_3$ (Aldrich, 99.5%) or $BaCO_3$ (Aldrich, 99.98%), Bi_2O_3 (Aldrich, 99.999%) and Nb_2O_5 (Aldrich, 99.9%), as described previously.[1] Preliminary X-ray powder diffraction measurements, using Cu-Kα radiation on a Siemens D-5000 diffractometer, did not reveal any impurity phases. The samples were then pressed into 13 mm diameter pellets. A number of pellets were heated in a muffle furnace at 600, 700, 800, 900, 1000, 1100 and 1200 °C for 4 h and then quenched to room temperature. The remaining samples were slowly cooled (5 K min^{-1}) to room temperature. Throughout this paper each sample is referred to by the cation and the temperature from which it was quenched, for example Sr700 indicates a sample of $SrBi_2Nb_2O_9$ quenched from 700 °C.

Variable temperature studies ($25 \leqslant T \leqslant 1000$ °C, 50 °C step) were conducted on both SrRT and BaRT using an Anton-Paar high temperature attachment on a Siemens D5000 diffractometer. Patterns were collected between $10° \leqslant 2\theta \leqslant 80°$ in 0.04° steps. Synchrotron powder X-ray diffraction data were collected using the Debye Scherrer camera at the Australian National Beamline Facility, Photon Factory, Japan.[16] Samples were loaded into 0.5 mm glass capillaries that were rotated during the measurements. All measurements were performed under vacuum to minimise air scatter. This diffractometer is equipped with an automatic sample changer capable of holding eight samples. The BAS2000 Fuji image plates are 20 cm × 40 cm and each covers 40° in 2θ. A thin strip *ca.* 0.5 cm wide is used to record each diffraction pattern, and by translating the image plate behind a Weissenberg screen it is possible to collect around 20 diffraction patterns on each image plate. In this work we placed five samples and a Si standard in the sample changer, so that it was possible to collect data at three wavelengths for each sample and standard without replacing the image plates. The diffraction patterns were recorded at *ca.* 0.85, 0.875 and 0.925 Å. These wavelengths were chosen to provide different scattering factors for Bi, since near the Bi absorption edge (0.924 Å) the complex scattering factor will be greatly enhanced.

The Rietveld refinement[17] was undertaken with the PC version of the program LHPM.[18] The background was defined by a fourth-order polynomial in 2θ and was refined simultaneously with the profile parameters. A pseudo-Voigt function was chosen to generate the profiles. An absorption correction using the algorithm described by Sabine[19] was also included. The values of f' and f'' for Bi used in the refinements were calculated using the program FPRIME.[20]

Structure refinement

The powder X-ray diffraction patterns, collected using our laboratory diffractometer, confirmed that the strontium oxides and all the barium oxides, except Ba1100 and Ba1200, were single phase Aurivillius type oxides. Heating $BaBi_2Nb_2O_9$ at or above 1100 °C resulted in partial decomposition and these samples were not further investigated. The strontium oxides were orthorhombic and all the peaks could be indexed in space group $A2_1am$, whilst the barium oxides adopted the archetypal $I4_1/mmm$ tetragonal cell.

The variable temperature X-ray diffraction studies on SrRT and BaRT demonstrate that the cells expand as the temperature was increased (Fig. 1 and Table 1). The two oxides have a similar degree of expansion over a comparable temperature range. While the variable temperature data, collected using non-monochromated Cu-Kα radiation, was not of sufficient quality for a detailed study of structural changes between 1000 and 25 °C it was adequate to obtain accurate cell parameters and volumes. Thus in addition to a major change in both oxides near 900 °C a number of smaller discontinuities are evident in Fig. 1 that are indicative of electronic and/or structural phase transitions. For example the Curie temperature of $SrBi_2Nb_2O_9$ is 420 °C and this may correspond to the discontinuity at about 400 °C.

The previously reported structural parameters for $ABi_2Nb_2O_9$ (A = Sr, Ba),[1,2] obtained by neutron diffraction methods, were used as starting models in the refinements using the X-ray diffraction data collected at three wavelengths. Initially it was assumed that the cations were fully ordered *i.e.* the Sr or Ba only occupy the perovskite A-type sites. The background, cell, profile, positional and isotropic displacement parameters of all atoms except the oxygen atoms were refined. The atomic displacement parameters of the crystallographically distinct oxygen atoms were constrained to be equal. Once convergence had been reached, disorder of the Bi and Sr or Ba atoms was considered. It was assumed that the Bi and A type cations occupy identical positions in the lattice and that the atomic displacements of the atoms on equivalent sites were equal. The occupancies of the sites were constrained so that both sites were fully occupied and the A : Bi stoichiometry was

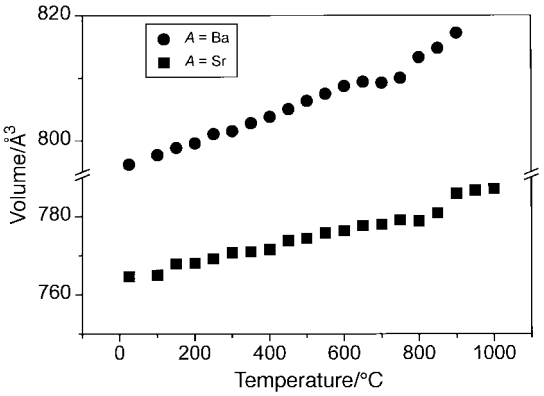

Fig. 1 Variation of the cell volume of $ABi_2Nb_2O_9$, (A = Sr, Ba) as function of temperature. The estimated standard deviations are smaller than the size of the symbols.

Table 1 Cell parameters for $SrBi_2Nb_2O_9$ and $BaBi_2Nb_2O$ as a function of temperature

	$SrBi_2Nb_2O_9$			$BaBi_2Nb_2O$	
T/ °C	a/Å	b/Å	c/Å	a/Å	c/Å
25	5.5193(7)	5.5164(7)	25.112(3)	3.9398(7)	25.647(5)
100	5.5196(7)	5.5190(7)	25.114(3)	3.9411(7)	25.679(5)
150	5.5276(7)	5.5247(7)	25.143(3)	3.9430(7)	25.691(5)
200	5.5279(7)	5.5250(7)	25.146(3)	3.9432(7)	25.712(5)
250	5.5302(7)	5.5273(7)	25.163(3)	3.9451(7)	25.735(5)
300	5.5346(7)	5.5317(7)	25.173(3)	3.9454(7)	25.746(5)
350	5.5355(7)	5.5326(7)	25.171(3)	3.9466(7)	25.771(5)
400	5.5374(7)	5.5344(7)	25.175(3)	3.9480(7)	25.785(5)
450	5.5378(7)	5.5449(7)	25.200(7)	3.9494(7)	25.806(5)
500	5.5452(7)	5.5422(7)	25.196(3)	3.9514(7)	25.822(5)
550	5.5486(7)	5.5456(7)	25.210(3)	3.9528(7)	25.840(5)
600	5.5504(7)	5.5474(7)	25.211(3)	3.9544(7)	25.858(5)
650	5.5532(7)	5.5503(7)	25.228(3)	3.9550(7)	25.872(5)
700	5.5538(7)	5.5509(7)	25.232(3)	3.9541(7)	25.879(5)
750	5.5566(7)	5.5537(7)	25.244(3)	3.9552(7)	25.889(5)
800	5.5570(7)	5.5553(7)	25.243(3)	3.9598(7)	25.934(5)
850	5.5600(7)	5.5572(7)	25.270(3)	3.9614(7)	25.960(5)
900	5.5705(7)	5.5694(7)	25.328(3)	3.9634(7)	26.011(5)
950	5.5716(7)	5.5687(7)	25.353(3)		
1000	5.5715(7)	5.5686(7)	25.366(3)		

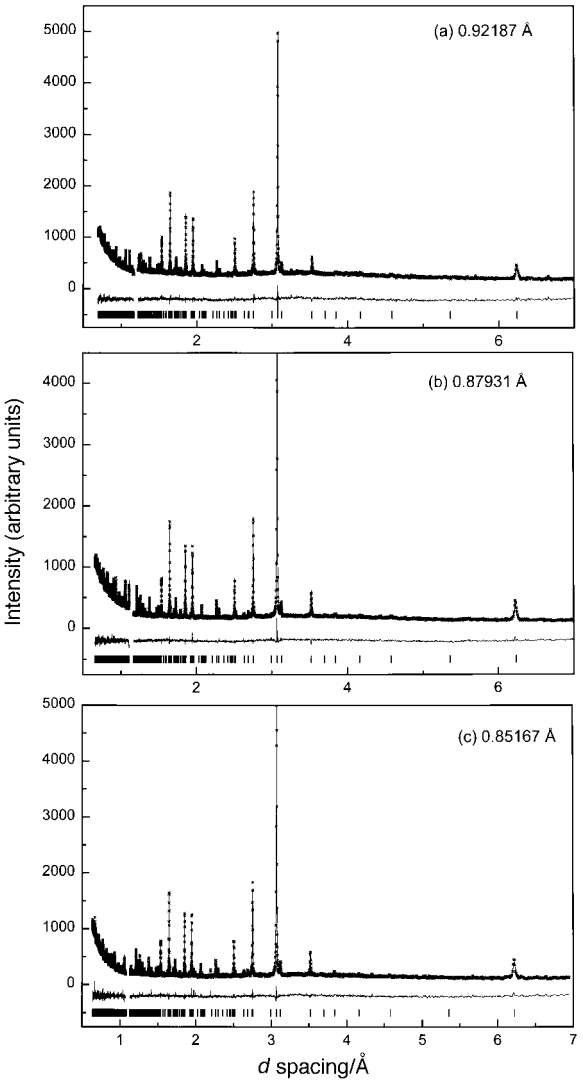

Fig. 2 Rietveld fit for synchrotron X-ray powder diffraction data of $SrBi_2Nb_2O_9$, quenched from 900 °C collected at (a) 0.92187, (b) 0.87931 and (c) 0.85167 Å. The crosses and solid line are the observed and calculated patterns respectively, while the difference profile and allowed reflection positions are shown underneath.

Table 2 Cell parameters and various measures of fit for $ABi_2Nb_2O_9$ (A = Sr, Ba) quenched from different temperatures

	T_{quench}/°C							
	25	600	700	800	900	1000	1100	1200
$SrBi_2Nb_2O_9$								
a/Å	5.5167(2)	5.5172(2)	5.5179(2)	5.5164(2)	5.5176(2)	5.5160(2)	5.5196(2)	5.5179(1)
b/Å	5.5137(2)	5.5149(2)	5.5147(2)	5.5141(2)	5.5152(2)	5.5126(2)	5.5168(2)	5.5135(1)
c/Å	25.0767(5)	25.0807(5)	25.0807(6)	25.0829(4)	25.0819(5)	25.0951(5)	25.0938(6)	25.1339(6)
V/Å^3	762.77(5)	763.12(5)	763.17(4)	762.96(3)	763.27(5)	763.08(3)	764.12(4)	764.64(3)
Sr/Bi 4(a)	89(1)/11(1)	89(1)/11(1)	90(1)/10(1)	88(1)/12(1)	89(1)/11(1)	86(1)/14(1)	87(1)/13(1)	84(1)/16(1)
Bi/Sr 8(b)	94(1)/6(1)	94(1)/6(1)	95(1)/5(1)	94(1)/6(1)	94(1)/6(1)	93(1)/7(1)	93(1)/7(1)	92(1)/8(1)
R_p(%)	2.77	4.25	4.39	4.43	2.97	3.62	4.46	3.56
R_{wp}(%)	5.83	7.32	7.21	7.21	6.07	6.72	7.51	7.19
GOF(%)	12.69	7.33	7.32	6.67	10.65	6.64	6.62	9.42
$BaBi_2Nb_2O_9$								
$a = b$/Å	3.9364(1)	3.9377(1)	3.9376(1)	3.9389(1)	3.9390(1)	3.9387(1)	—[a]	—[a]
c/Å	25.6386(5)	25.6287(5)	25.6301(5)	25.6359(5)	25.6364(5)	25.6406(5)		
V/Å^3	397.28(1)	397.39(1)	397.39(1)	397.74(1)	397.77(1)	397.78(1)		
Ba/Bi 2(b)	85(2)/15(2)	85(2)/15(2)	85(2)/15(2)	84(2)/16(2)	84(2)/16(2)	80(2)/20(2)		
Bi/Ba 4(e)	92(2)/8(2)	92(2)/8(2)	92(2)/8(2)	92(2)/8(2)	92(2)/8(2)	90(2)/10(2)		
R_p(%)	3.53	3.74	3.31	3.39	3.03	3.01		
R_{wp}(%)	7.50	6.16	5.94	5.67	5.34	6.38		
GOF(%)	19.20	6.77	10.34	7.69	7.29	5.77		

[a]Partially decomposed.

maintained. Values of the cell parameters and various measures of fit from the refinements are listed in Table 2, while the positional and atomic displacement parameters are listed in Table 3. An example of a refinement is shown in Fig. 2.

Discussion

The powder diffraction patterns clearly demonstrate that thermal annealing does not alter the bulk structures of $BaBi_2Nb_2O_9$ and $SrBi_2Nb_2O_9$. As is illustrated in Fig. 3 the cell volume for both complexes is dependent on the thermal annealing conditions and increases as the temperature from which the sample is quenched increases, Table 2. This increase in the cell parameters mimics that observed in the temperature dependent studies. A similar, although less dramatic, change is found in $PbBi_2Nb_2O_9$.[14] For both $BaBi_2Nb_2O_9$ and $SrBi_2Nb_2O_9$ the increase in the cell volume is not isotropic, rather the rate of increase of the c axis is largest in both

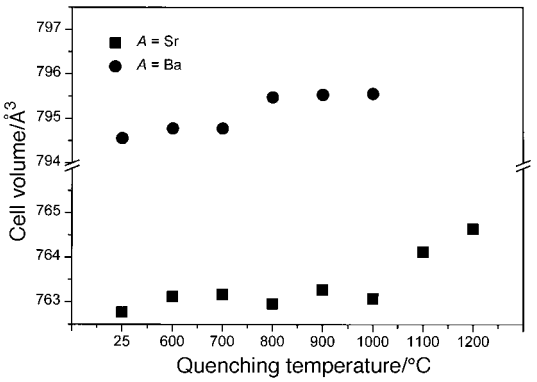

Fig. 3 Cell volume of $ABi_2Nb_2O_9$, (A = Sr, Ba) quenched from different temperatures. For ease of comparison $2V$ is plotted for $BaBi_2Nb_2O_9$. The estimated standard deviations are smaller than the size of the symbols.

Table 3 Positional and isotropic atomic displacement parameters for $ABi_2Nb_2O_9$ (A = Sr, Ba) quenched from different temperatures[a]

	T_{quench}/°C							
	25	600	700	800	900	1000	1100	1200
$SrBi_2Nb_2O_9$								
Sr y	0.241(2)	0.247(2)	0.241(2)	0.244(2)	0.240(2)	0.244(2)	0.245(2)	0.246(2)
Sr U_{iso}/Å^2	0.013(1)	0.015(1)	0.022(1)	0.023(1)	0.022(1)	0.021(1)	0.023(1)	0.027(1)
Bi x	0.473(2)	0.473(2)	0.474(2)	0.471(2)	0.475(2)	0.472(2)	0.470(2)	0.473(2)
y	0.733(7)	0.733(7)	0.734(7)	0.732(7)	0.733(7)	0.732(7)	0.733(7)	0.734(7)
z	0.2011(1)	0.2010(1)	0.2010(1)	0.2010(1)	0.2014(1)	0.2010(1)	0.2010(1)	0.2012(1)
Bi U_{iso}/Å^2	0.032(1)	0.052(1)	0.052(1)	0.053(1)	0.062(1)	0.047(1)	0.045(1)	0.067(1)
Nb x	0.471(1)	0.470(1)	0.470(1)	0.470(1)	0.470(1)	0.469(1)	0.469(1)	0.472(1)
y	0.750(1)	0.751(1)	0.747(1)	0.750(1)	0.751(1)	0.750(1)	0.748(1)	0.752(1)
z	0.4133(1)	0.4136(1)	0.4136(1)	0.4136(1)	0.4132(1)	0.4134(1)	0.4133(1)	0.4131(1)
Nb U_{iso}/Å^2	0.006(1)	0.010(1)	0.012(1)	0.013(1)	0.012(1)	0.0121(1)	0.013(1)	0.015(1)
O U_{iso}/Å^2	0.023(1)	0.055(1)	0.072(1)	0.073(1)	0.049(1)	0.047(1)	0.043(1)	0.047(1)
$BaBi_2Nb_2O_9$								
Ba U_{iso}/Å^2	0.026(2)	0.040(2)	0.040(2)	0.042(2)	0.050(2)	0.052(2)		
Bi z	0.2026(1)	0.2027(1)	0.2021(1)	0.2029(1)	0.2023(1)	0.2028(1)		
Bi U_{iso}/Å^2	0.030(1)	0.056(1)	0.067(1)	0.060(1)	0.062(1)	0.062(1)		
Nb z	0.0887(1)	0.0882(1)	0.0883(1)	0.0884(1)	0.0884(1)	0.0886(1)		
Nb U_{iso}/Å^2	0.003(1)	0.007(1)	0.015(1)	0.010(1)	0.010(1)	0.016(1)		
O U_{iso}/Å^2	0.061(5)	0.057(3)	0.066(3)	0.055(3)	0.088(2)	0.064(3)		

[a]$SrBi_2Nb_2O_9$ $A2_1am$: Sr on 4a (0, y, 0) Bi on 8b (x, y, z), Nb on 8b (x, y, z), O(1) on 4a (0.462, 0.211, 0), O(2) on 8b (0.470, 0.798, 0.3410), O(3) on 8b (0.738, −0.005, 0.2500) O(4) on 8b (0.673, 0.967, 0.0849) and O(5) on 8b (0.729, 0.976, 0.5707); $BaBi_2Nb_2O_9$ $I4_1/mmm$ Ba on 2b (1/2, 1/2, 0) Bi on 4e (1/2, 1/2, z), Nb on 4e (0, 0, z) O(1) on 2a (1/2, 1/2, 1/2), O(2) on 4d (0, 1/2, 1/4), O(3) and O(4) on 4e (0, 0, 0.1603) and 8g (0, 1/2, 0.07818).

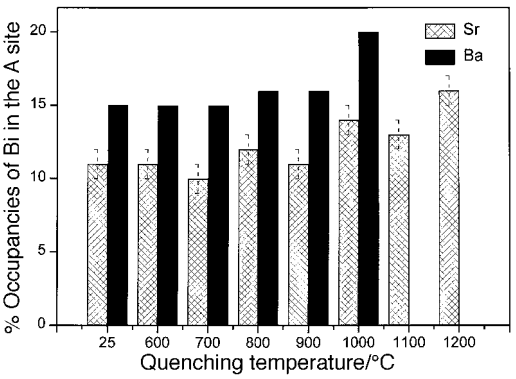

Fig. 4 Percentage occupancy of Bi in the A site of $ABi_2Nb_2O_9$, (A = Sr, Ba) quenched from different temperatures.

oxides. In orthorhombic $SrBi_2Nb_2O_9$ the a/b ratio is essentially independent of the quenching temperature and this increases slightly on increasing temperature.

The positional parameters of the heavy atoms in both compounds are independent of quenching temperature, Table 3, and are in good agreement with values reported previously using powder neutron diffraction data. Because of the weak scattering power of the lighter oxygen atoms, only the atomic displacement parameters of these were varied during the structural refinements and these yielded small positive numbers in all cases suggesting that the positions of these atoms were not significantly altered by the cooling conditions.

The refined occupancy parameters demonstrate there is some mixed occupancy of the Bi and A-type cation sites and that the extent of this mixing is dependent on the quenching temperature. In general the extent of disorder is greatest in $BaBi_2Nb_2O_9$ where 15–20% of the Ba^{2+} cations are in the $[Bi_2O_2]$ layers compared to 10–16% of Sr^{2+} in $SrBi_2Nb_2O_9$. In both cases the disorder increases with increasing annealing temperature, Fig. 4. The extent of this disorder is considerably less than we observed in $PbBi_2Nb_2O_9$ where up to 50% of the Pb cations are in the $[Bi_2O_2]$ layers.[14] The increased occupancy of the $[Bi_2O_2]$ layers by the A-type cations upon high temperature annealing mirrors the increase in the cell volumes. This, as is discussed in more detail below, is related to the increasing ability of the Bi_2O_2 layer to incorporate the larger Sr^{2+} and Ba^{2+} cations.

It is interesting to compare the tendency for the three oxides, $ABi_2Nb_2O_9$ (A = Sr, Ba and Pb), to incorporate A type cations into the $[Bi_2O_2]$ layers. It has been suggested that the need to overcome the overbonding of the A-type cations and underbonding in the Bi sites is a significant factor in tuning the structure of these types of oxides[2] and may be a major contribution to the observed disorder. This explains the greater disorder in the Ba complex relative to the Sr complex, Table 2 and Fig. 4, and is reflected in the valence bond sum calculations. The VBS for the A site cation are, for Ba 3.02 and 2.83 for fully ordered and disordered distributions respectively; whilst for Sr the corresponding values are 2.43 and 2.41. The VBS for the Bi site are, for the ordered distribution in $SrBi_2Nb_2O_9$ and $BaBi_2Nb_2O_9$ 2.79 and 2.57 respectively, whilst for disordered distribution they are 2.80 and 2.71. The still greater disorder in $PbBi_2Nb_2O_9$ is then readily explained by recalling that both Bi^{3+} and Pb^{2+} have sterochemically active $6s^2$ electrons. Blake *et al.* further proposed that the ideal value of the bond valence for the divalent cation in an Aurivillius structure is in the region 2.3–2.4. The effective VBS value of the cations in the Ba site in $BaBi_2Nb_2O_9$ is higher than this value and, in principle, this can be reduced by increasing disorder of Ba and Bi over the perovskite and Bi_2O_2 layers. The results, however, offer no indication of any further increase in the disorder with increasing quenching temperature. Thus there must be a mechanism to prevent further disorder of cations over both layers.

The disorder of Sr or Ba and Bi over both layers stabilises the perovskite slabs, but destabilises the Bi_2O_2 layers, since both Sr and Ba lack lone pair electrons. The present results show that the Bi_2O_2 layer can tolerate *ca.* 20% of Sr/Ba disorder without significant loss of structural stability. The slight increase in the degree of cation disorder in $ABi_2Nb_2O_9$ (A = Sr, Ba) with increasing temperature mimics the change in the cell volume observed in the *in situ* powder diffraction measurements. With increasing temperature the cell volume expands and this favours the incorporation of the larger Sr and Ba cations into the Bi_2O_2 layers. This arrangement of cations is retained, at least in part, upon quenching.

In conclusion both Sr and Ba can occupy the Bi sites in $ABi_2Nb_2O_9$ (A = Sr, Ba). The change in the degree of disorder is strongly related to the change in the cell volume, which in turn is related to the quenching temperature. The degree of disorder observed in both complexes is much lower that that observed in $PbBi_2Nb_2O_9$ due to the absence of lone pair electrons in Sr^{2+} and Ba^{2+}. More detailed studies of the high temperature structures are required to better understand this relationship.

Acknowledgments

This work has been supported by the Australian National Beamline Facility. The assistance of Drs Cookson and Foran in collecting the synchrotron diffraction data and that for Maree Anast (UTS) in recording the variable temperature X-ray diffraction data is gratefully acknowledged.

References

1 Ismunandar, B. J. Kennedy, Gunawan and Marsongkohadi, *J. Solid State Chem.*, 1996, **126**, 135.
2 S. M. Blake, M. J. Falconer, M. McCreedy and P. Lightfoot, *J. Mater. Chem.*, 1997, **7**, 1609.
3 L. Korzunova, *Ferroelectrics*, 1992, **134**, 175.
4 D. J. Buttrey, T. Vogt, U. Wildgruber and W. R. Robinson, *J. Solid State Chem.*, 1994, **111**, 118.
5 K. V. R. Prasad and K. B. R. Varma, *Mater. Chem. Phys.*, 1994, **38**, 406.
6 B. Aurivillius, *Ark. Kemi.*, 1949, **1**, 463.
7 E. C. Subbarao, *J. Am. Ceram. Soc.*, 1962, **45**, 166.
8 R. E. Newnham, R. W. Wolfe and J. F. Dorrian, *Mater. Res. Bull.*, 1971, **6**, 1029.
9 T. Rentschler, *Mater. Res. Bull.*, 1997, **32**, 351.
10 P. Millan, A. Castro and J. B. Torrance, *Mater. Res. Bul.*, 1993, **28**, 117.
11 P. Millan, A. Ramirez and A. Castro, *J. Mater. Sci. Lett.*, 1995, **14**, 1657.
12 A. Castro, P. Millan, M. J. Martinez-Lope and J. B. Torrance, *Solid State Ionics*, 1993, **63–65**, 897.
13 A. Castro, P. Millan and R. Enjalbert, *Mater. Res. Bull.*, 1995, **30**, 871.
14 Ismunandar, B. J. Kennedy and B. A. Hunter, *Solid State Ionics*, 1998, **112**, 281.
15 R. B. Von Dreele, in *The Rietveld Method*, ed. R. A. Young, Oxford University Press Inc., New York, 1st edn., 1993.
16 T. M. Sabine, B. J. Kennedy, R. F. Garrett, G. J. Foran and D. J. Cookson, *J. Appl. Crystallogr.*, 1995, **28**, 513.
17 H. M. Rietveld, *J. Appl. Crystallogr.*, 1969, **2**, 65.
18 R. J. Hill and C. J. Howard, *Australian Atomic Energy Commision Report No. M112*, AAEC (now ANSTO), Lucas Heights Research Laboratories, 1986.
19 T. M. Sabine, B. A. Hunter and W. R. Sabine, *J. Appl. Crystallogr.*, 1998, **31**, 47.
20 D. T. Cromer and D. A. Liberman, *Acta Crystallogr., Sect. B*, 1981, **47**, 267.
21 R. D. Shannon, *Acta Crystallogr., Sect. A*, 1976, **32**, 751.

Paper 8/06760K